Clay Minerals (2024), **59**, 127–135
doi:10.1180/clm.2024.13

CAMBRIDGE UNIVERSITY PRESS

Article

Facile preparation of sepiolite-based composites and their antibacterial/rheological properties

Yizhi Jiang[1], Zongfan Peng[2], Yongwen Yang[3], Yuqin Li[2], Yufang Tang[2] and Yanhuai Ding[1]

[1]School of Mechanical Engineering and Mechanics, Xiangtan University, Hunan, China; [2]School of Chemical Engineering, Xiangtan University, Hunan, China and [3]Department of Clinical Laboratory, Xiangya Hospital, Central South University, Changsha, Hunan, China

Abstract

Natural sepiolite has great potential for application in wound healing, haemostasis and medicines. This paper introduces a versatile solid-state sintering technique for preparing sepiolite-based nanocomposites with enhanced antibacterial properties, and the physical, structural, rheological and antibacterial properties of which were determined to be enhanced. The incorporation of nanosized Ag and metal oxides into sepiolite composites results in a notable improvement in their antibacterial efficacy against *Escherichia coli* and *Staphylococcus aureus* in comparison to the unmodified sepiolite. With a low silver content of just 5%, the sepiolite–Ag composite achieves an antibacterial rate of ~100%. Furthermore, the rheological properties exhibited by the sepiolite composites are noteworthy, suggesting their suitability for use in wound-dressing applications due to their exceptional workability. The methodology employed in this research has the potential to offer a viable substitute for the production of economical and effective natural antibacterial nanocomposites.

Keywords: Antibacterial properties; composites; metal oxides; rheological behaviour; sepiolite

(Received 24 February 2024; revised 21 April 2024; accepted 21 April 2024; Accepted Manuscript online: 24 April 2024)

Sepiolite (Sep), a natural fibrous clay mineral, is characterized by a significant external surface area, which presents promising prospects for the development of nanocomposites (Kose *et al.*, 2005; Jiang *et al.*, 2020, 2021, 2024). The structure of Sep comprises alternating blocks and channels aligned along the fibre direction (Alves *et al.*, 2020; Zhou *et al.*, 2023). Within its framework, two tetrahedral silica sheets encase a central octahedral sheet that contains magnesium, forming the fundamental unit of the Sep structure. The presence of numerous Si-OH groups on the surface, as a result of the tetrahedral silica sheets, endows Sep with a variety of applications in fields such as adsorption, catalysis and energy storage and conversion (Vilarrasa-García *et al.*, 2017; Junior *et al.*, 2020; Huang *et al.*, 2024). Nevertheless, the raw Sep's specific surface area was insufficient to satisfy the demands of practical applications. To address this, various methods, including acid treatment, heat treatment and surface modification, have been utilized to increase the specific surface area and, consequently, enhance the physical properties of Sep (Dutta & Devi, 2021; Pang *et al.*, 2022; Wu *et al.*, 2017). However, the aforementioned methods for modifying Sep often require reactions to be carried out in a solution, and such processes are cumbersome, time-consuming and not environmentally friendly.

Amongst the techniques mentioned, acid treatment is commonly used to increase the surface area and reduce impurities in Sep (Franco *et al.*, 2014; Valentín *et al.*, 2007). However, this method is not environmentally friendly as it can generate effluents. Fabricating Sep composites presents an alternative approach to improve the physical properties of Sep. The *in situ* production of crystalline nanoparticles on the Sep surface has been widely reported in recent literature (Aranda & Ruiz-Hitzky, 2018; Ma & Zhang, 2016). The development of Sep-based nanoarchitectures holds great promise for a range of applications in next-generation functional materials. Various Sep–metal oxide composites have been synthesized using methods such as the sol–gel process (Zhang *et al.*, 2011), solvothermal synthesis (Liu *et al.*, 2018) and other wet chemical techniques (Song *et al.*, 2023). For example, Sep–TiO_2 nanocomposites were synthesized by microwave hydrothermal treatment, which produced relatively uniformly distributed TiO_2 particles on the Sep surface without visible aggregation (Zhou *et al.*, 2018). Additionally, Sep–Cu_2O–Cu ternary composites have been successfully synthesized using a hydrothermal method, with Sep serving as a nonremovable template (Zhou *et al.*, 2022). These composites have demonstrated excellent electrochemical performance as anodes in Li-ion batteries. Fe_2O_3–Sep magnetic materials, synthesized *via* chemical co-precipitation, have potential applications as effective adsorbents for the removal of anionic dyes, such as Congo Red, from aqueous solutions (Wang *et al.*, 2018). However, many of these synthesis methods rely on the use of harmful chemicals and involve complex fabrication processes (Uygun *et al.*, 2023). Consequently, there is an urgent need to develop greener techniques that are cost-effective, efficient and environmentally friendly for the preparation of Sep–metal oxide composites.

Today, increased interest has been focused on various clay groups for fabricating wound-dressing materials (Tavakoli, 2017; Dutta & Devi, 2021; Hardt *et al.*, 2021; Huang *et al.*, 2024).

Corresponding authors: Yanhuai Ding; Email: yhding@xtu.edu.cn; Yongwen Yang; Email: yongwen1007@csu.edu.cn

Cite this article: Jiang Y, Peng Z, Yang Y, Li Y, Tang Y, Ding Y (2024). Facile preparation of sepiolite-based composites and their antibacterial/rheological properties. *Clay Minerals* **59**, 127–135. https://doi.org/10.1180/clm.2024.13

Sep, due to its excellent absorption capacity for exudates, has broad potential applicability for wound dressings. However, powdered Sep cannot be directly used for wound treatment. It is reported in the literature that Sep is commonly combined with materials such as chitosan and gelatin to prepare wound dressings (Liu *et al.*, 2016). This process requires complex techniques and is not suitable for large-scale preparation. Therefore, developing a large-scale green preparation method for Sep wound dressings remains a challenge.

Recently, we reported on a Sep composite material for rapid haemostasis (Jiang *et al.*, 2023). Zeolite-based nanomaterials have been proven to be one of the most effective haemostatic materials due to their high water-adsorption capability and ability to speed up coagulation in the blood (Zhang *et al.*, 2021b; Zheng *et al.*, 2023). However, zeolite-based haemostatic materials may cause potential tissue injury due to their exothermic physical effects, greatly limiting their applicability as haemostatic agents. Compared with commercial zeolite materials, the current Sep composite exhibits competitive haemostatic properties without producing exothermic reactions.

Of key importance will be developing green technologies for the large-scale preparation of Sep composite materials. In this study, we propose a versatile solid-state sintering method for the preparation of Sep-based nanocomposites with improved antibacterial properties. This method is notable for its safety, cost-effectiveness and time efficiency. Utilizing readily decomposable metal acetates, nanoparticles are generated *in situ* on the Sep surface at low sintering temperatures. The resulting Sep-based composites demonstrate significantly improved antibacterial properties when compared to the raw Sep materials. By employing this method, the unique properties of Sep are leveraged to create nanocomposites with a broader range of applications, particularly in the field of antibacterial materials and wound dressings. The low-temperature sintering process not only ensures the safety and environmental friendliness of the procedure, but also reduces overall production costs and times, making this approach a viable option for large-scale applications.

Experimental

Materials and chemicals

Sep powders (purity ~70%) were provided by Xiangtan Sepiolite Technology Co., Ltd (Hunan, China). Silver acetate (CH_3COOAg), copper acetate monohydrate ($C_4H_6CuO_4{\cdot}H_2O$), zinc acetate ($C_4H_6O_4Zn$) and sodium chloride (NaCl) were purchased from Macklin Chemical Co., Ltd. Tryptone, yeast, *Escherichia coli*, agar and *Staphylococcus aureus* were provided by Xiangya Hospital (Hunan, China). All of the materials and chemicals were used without further purification.

Preparation of materials

In this paper, we proposed a universal solid-state sintering method for the preparation of Sep-based nanocomposites. Firstly, Sep powders and CH_3COOAg, $C_4H_6CuO_4$ and $C_4H_6O_4Zn$ were mixed in particular proportions (9.00:1.00, 9.00:1.74 and 9.00:1.53, respectively). This mixture was then placed into a ball-milling tank and further mixed for 10 min at 500 rpm. Subsequently, the resulting powder was transferred into a muffle furnace and heated at a rate of 4°C min^{-1} to a final temperature of 500°C, where it was maintained for a duration of 5 h. Upon completion of the heating process, the furnace was allowed to cool down naturally to room temperature. The final product that was obtained after this cooling process was then ball-milled for an additional 10 min at 500 rpm. The resulting samples were designated as Sep/Ag, Sep/CuO and Sep/ZnO, corresponding to the respective metal oxides incorporated into the Sep matrix.

Characterization of materials

Following gold sputtering, the samples were examined using a field-emission scanning electron microscope (FE-SEM; ZEISS Sigma-300). The structural characteristics of the composites were analysed by X-ray diffraction (XRD) using a Rigaku SmartLab SE X system. Transmission electron microscopy (TEM) images were obtained using a JEOL JEM-F200 microscope. The antibacterial activities of the composites were evaluated using *E. coli* and *S. aureus* as model bacterial strains. Further details are provided in the Supplementary Materials.

Rheological experiments

For medical materials and wound dressings, good rheological properties can ensure the conformity of the wound dressing to the wound surface during application, and they can also affect the moisture retention capability of the wound dressing. In the development of new medical materials, it is essential to consider their rheological characteristics comprehensively to achieve optimal therapeutic outcomes and patient experience. Rheological experiments on the material were performed using an Anton Paar MCR 301 rheometer. The material was mixed with water to form a sample with flow-like viscosity, and a 25 mm-diameter cone-plate geometry was utilized for the tests. In the shear rate-viscosity test, the shear rate was varied over a range from 10^{-2} to 10.0 (s^{-1}). For the dynamic strain sweep, the strain amplitude was incrementally increased from 0.1% to 100%, with the frequency maintained at 5.0 Hz. The thixotropy test involved subjecting the sample to a 1% strain for 120 s, followed by an 80% strain for 60 s, both at a frequency of 5.0 Hz. This cyclic procedure was repeated a total of seven times. Throughout the testing, the environmental conditions were meticulously controlled, with the temperature set at 25°C and the relative humidity maintained at 50%.

Results and discussion

The schematic representation of the Sep-based composite preparation process is depicted in Fig. 1. The natural tendency of Sep fibres to agglomerate significantly impacts their dispersibility within composites (Chivrac *et al.*, 2010; García *et al.*, 2011; Zhou *et al.*, 2023). In this study, precursors were synthesized by ball-milling pristine Sep powder in the presence of solid metal acetates. The inclusion of metal acetates enhances the dispersibility of the Sep fibres by reducing the interactions between them. Consequently, the Sep fibres act to curb the growth of nanoparticles within the composites. Following the heat-treatment process, a secondary ball-milling step is conducted to further refine the particle size of the Sep-based composites. This methodology offers several notable advantages. Firstly, the preparation of the Sep-based composites does not require the use of solvents or water. Secondly, the entire preparation process is significantly more time-efficient and cost-effective compared to traditional wet chemical synthesis methods.

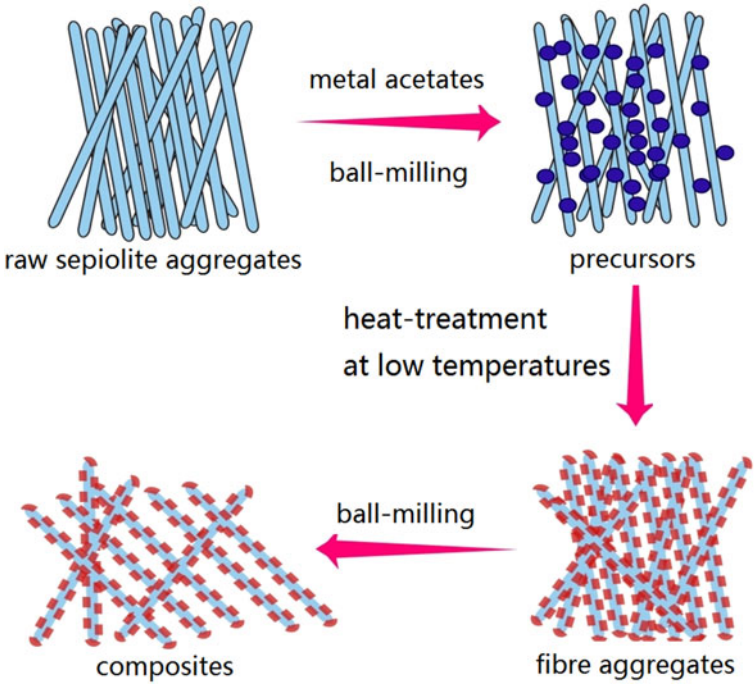

Figure 1. Schematic diagram of the preparation procedure for the Sep-based composites.

The SEM images of the as-prepared raw Sep and the Sep-based nanocomposites are presented in Fig. 2. The raw Sep displays a fibrous morphology with fibre diameters ranging from ~20 to 30 nm, as depicted in Fig. 2a. Some of the Sep fibres are stacked to form sheet-like structures. The presence of impurities, primarily calcite and talc, in the Sep clay results in a significant number

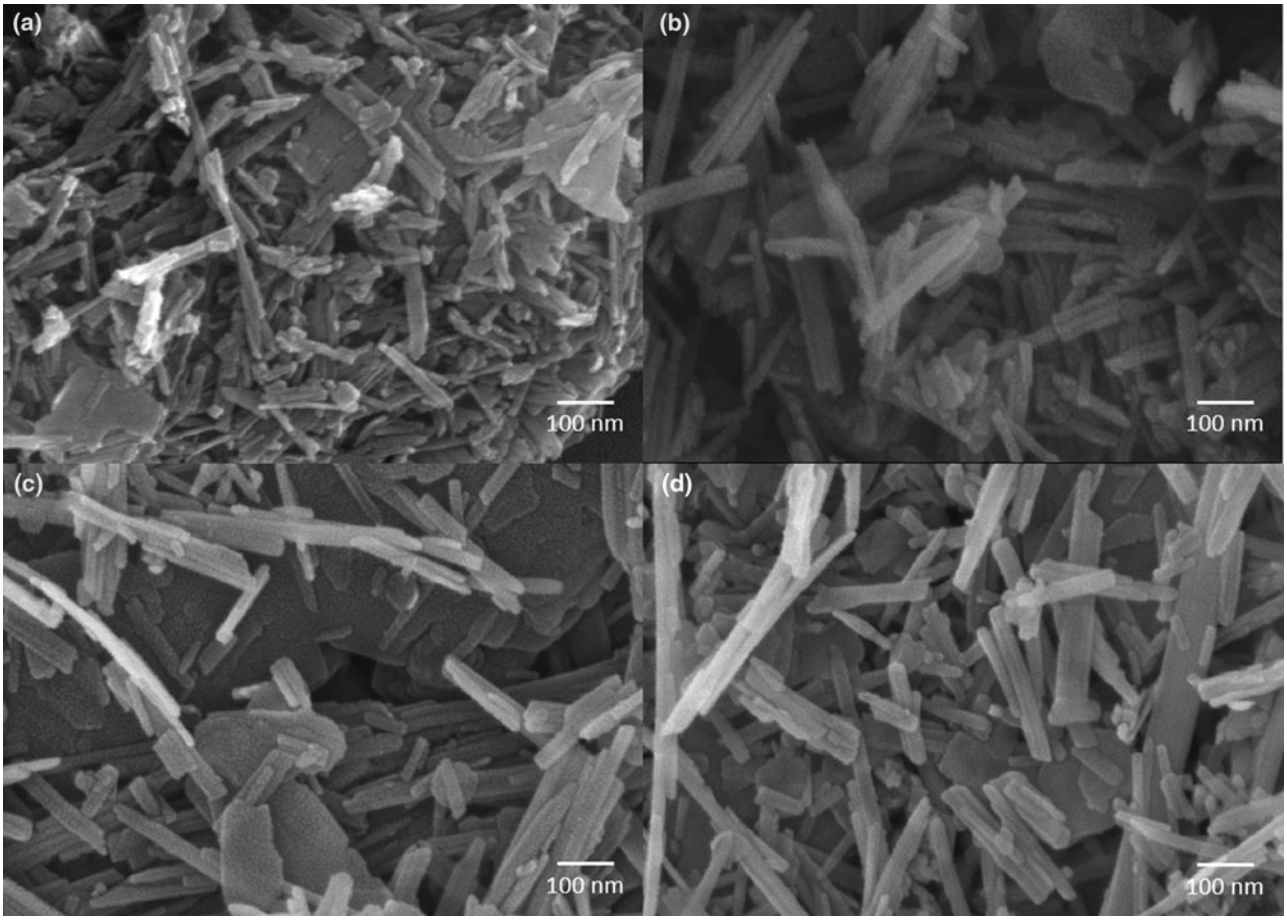

Figure 2. SEM images of the as-prepared raw Sep and Sep-based nanocomposites. (a) Sep, (b) Sep/Ag, (c) Sep/CuO, (d) Sep/ZnO.

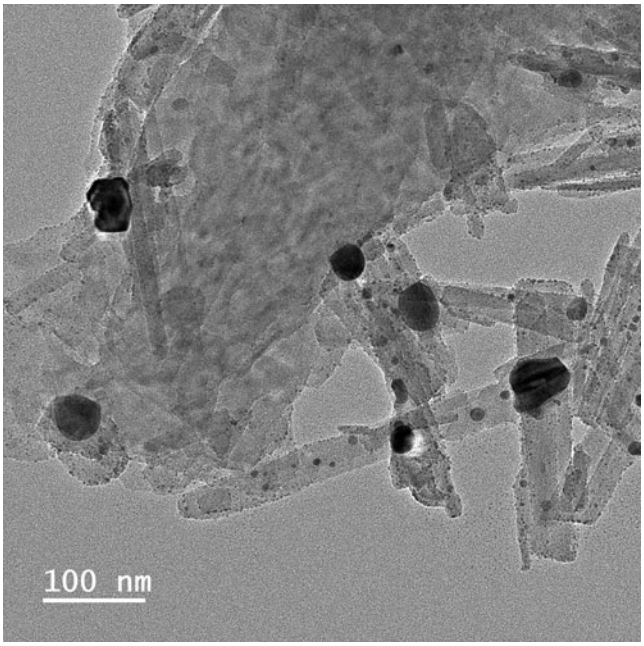

Figure 3. TEM image of the as-prepared Sep/Ag composites.

of nanoparticles being observable within the raw Sep sample. As shown in Fig. 2b, the Sep/Ag composites exhibit a fibrous morphology that closely resembles the structure of the pristine Sep. Following heat treatment, the fibrous morphology of the composites becomes more distinct. However, the presence or absence of Ag nanoparticles within the composites could be definitively ascertained. The Sep/CuO and Sep/ZnO composites, as illustrated in Fig. 2c,d, display morphological features that are similar to those observed in the Sep/Ag composites. This consistency suggests that the reaction mechanism proposed earlier aligns well with the observed experimental findings. TEM characterization was employed to confirm the morphology of the Sep-based composites. For instance, a substantial number of Ag nanoparticles are observable in the TEM images of the Sep/Ag composites, as depicted in Fig. 3. The majority of these Ag nanoparticles are found to be tightly affixed to the surface of the Sep fibres. The particle-size analysis is presented in Fig. S2. The average diameter of the nanoparticles, as measured according to Fig. S2, is ~8 nm. It is known that Ag nanoparticles with smaller particle sizes exhibit more potent antibacterial effects (Zhang *et al.*, 2021a). These findings suggest that the Sep fibres effectively restricted the growth of Ag nanoparticles, as postulated in the mechanism analysis. In the high-resolution TEM image (Fig. S1), the lattice spacing of 0.238 nm, corresponding to the (111) plane of the Ag nanoparticles, is clearly discernible (Chen *et al.*, 2016). These results confirm that the synthesis of ultrafine Ag nanoparticles was successful, as anticipated.

The crystal structures of the composites were further investigated by XRD analysis, as shown in Fig. 4. The diffractogram of the pure Sep exhibits the characteristic reflections of the unaltered microfibrous clay. The reflections at 7.2°2θ, 20.6°2θ, 26.6°2θ and 35.0°2θ correspond to the primary diffractions of the (110), (131), (040) and (400) planes of Sep (Jiang *et al.*, 2021), respectively. After modification, the characteristic diffraction peaks of Sep can still be observed, indicating that the crystal structure of Sep has not been destroyed. The characteristic XRD peaks of ZnO, CuO and Ag nanoparticles are found in the traces (Ding *et al.*, 2019, 2023). The XRD analysis demonstrates that the approach proposed in this work could be successfully used to prepare Sep-based composite. The energy-dispersive spectroscopy (EDS) analysis of the as-prepared composites is shown in Figs S3–S5. Ag, Cu and Zn elements can be detected in the composites. The elemental analysis indicates that the elemental content (>95%) in the as-prepared composite materials is significantly higher than that in the materials prepared using the hydrothermal method, indicating that the solid-phase sintering technology we proposed is more efficient. The reason is that, during the solid-phase sintering process, elements such as Ag, Cu and Zn are essentially not lost.

Sep holds significant potential for the development of sustainable antibacterial materials suitable for applications in food packaging, cosmetics, drug delivery systems and implantable devices (Lisuzzo *et al.*, 2020; Yang & Wang, 2022). However, raw Sep materials have been found to be ineffective against bacteria such as *E. coli* and *S. aureus* (Benli & Yalın, 2017). A particularly

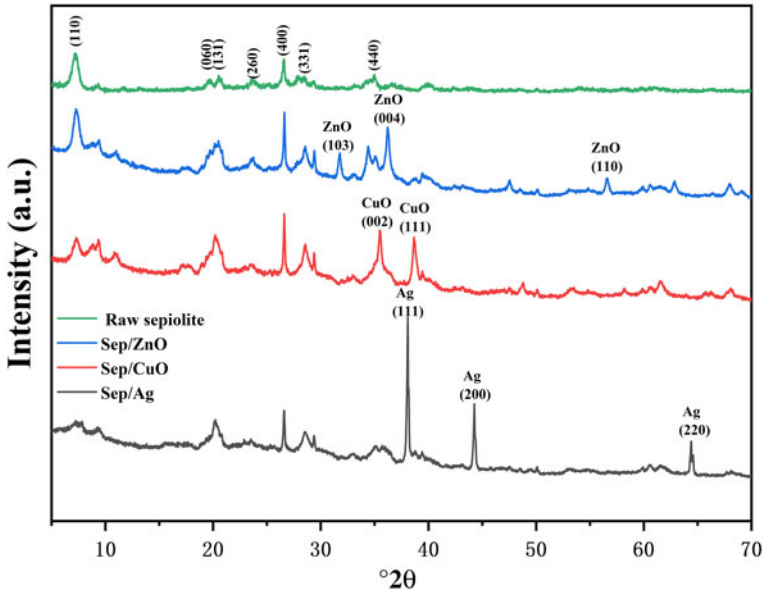

Figure 4. XRD traces of the as-prepared Sep-based composites.

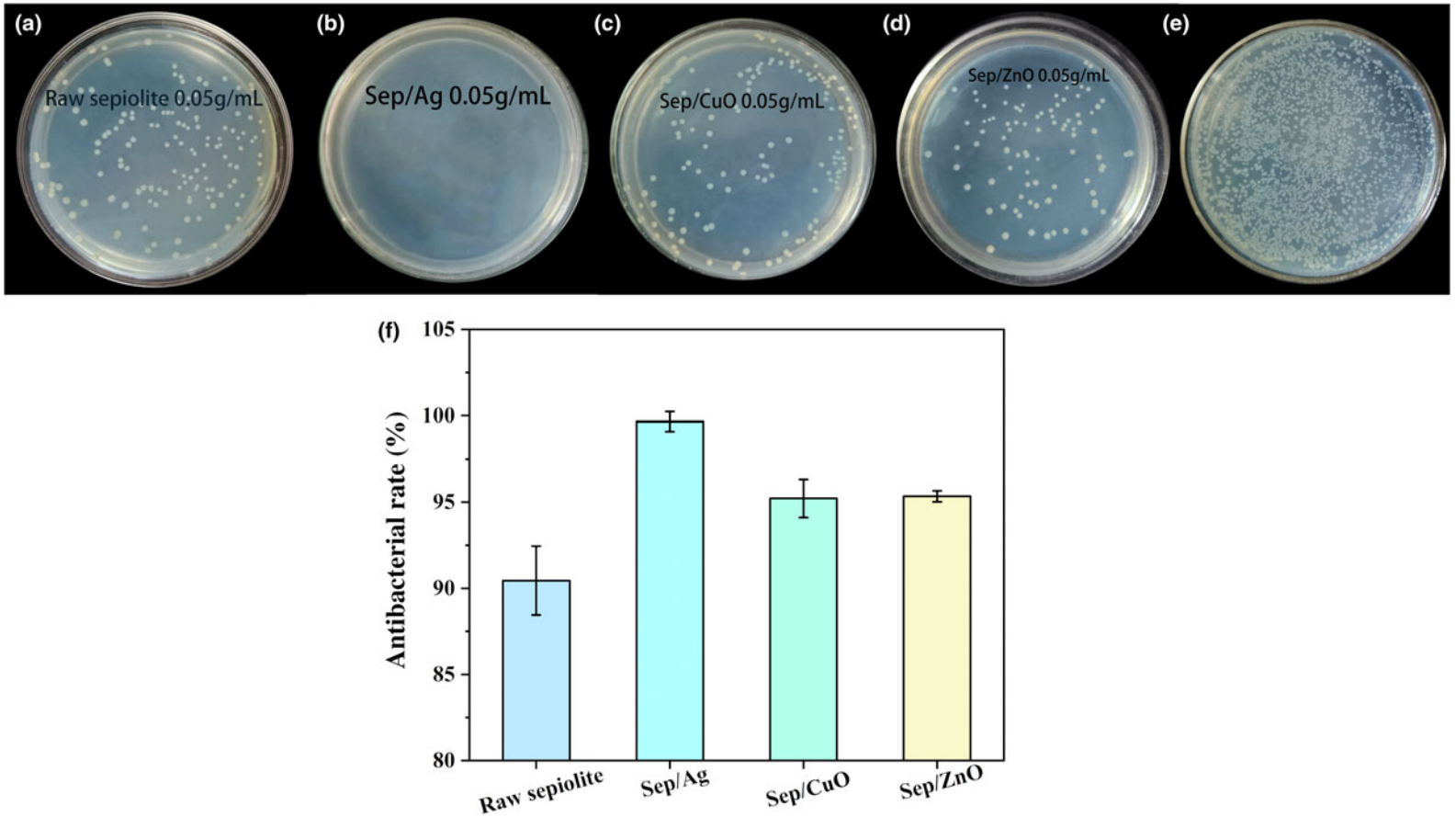

Figure 5. Antimicrobial activity of Sep and its composites towards *E. coli*. (a) Sep, (b) SEP/Ag, (c) Sep/CuO, (d) Sep/ZnO, (e) control group, (f) calculated antibacterial rate.

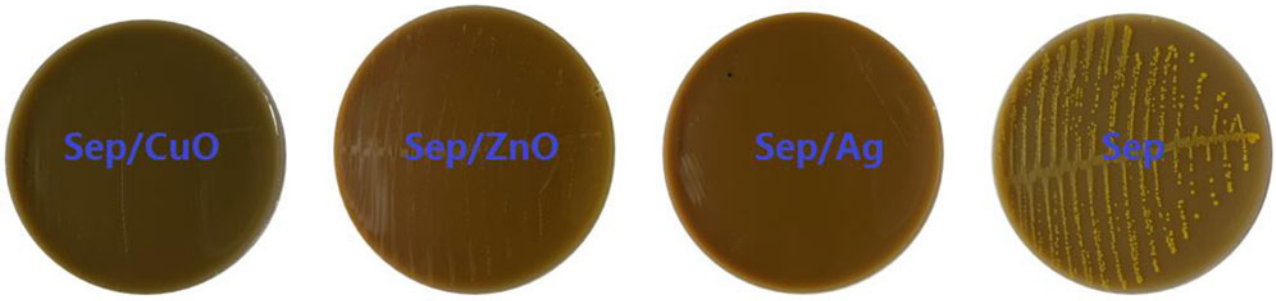

Figure 6. Antimicrobial activity of Sep and its composites towards *S. aureus*.

effective strategy is the combination of Sep with nanoparticles such as Ag and Cu (Esteban-Cubillo *et al.*, 2006; Benli & Yalın, 2017; Díez *et al.*, 2017). The antimicrobial activity of Sep and its composites against *E. coli* (ATCC 25922) is illustrated in Fig. 5a–e. The raw Sep showed poor antibacterial capability against *E. coli* when compared to the untreated control group, which is in line with previous findings. Typically, the surfaces of Sep nanofibres carry a negative charge (Dikmen *et al.*, 2012), which is neutralized by counterions and water molecules. From this perspective, there is a state of mutual exclusivity between Sep and bacteria. Therefore, it is hypothesized that surface complexation occurs between the bacteria and the surface hydroxyl groups of Sep. Upon modification with nanoparticles, the Ag-modified composites displayed the most potent antibacterial capabilities, followed by those modified with CuO and ZnO. The calculated antibacterial rates for the composites are depicted in Fig. 5f. The results indicate that the antibacterial rate of the Sep/Ag composite approaches ~100%. Given the low contents of Ag, CuO and ZnO in the composites (estimated at ~5%), the observed antibacterial capabilities of the prepared samples are remarkable.

The antimicrobial activity of Sep and its composites against *S. aureus* (ATCC 29213) is shown in Fig. 6. The composites exhibited similar antimicrobial activity against *S. aureus* as that against *E. coli*. Amongst the four samples, the Ag-modified composites demonstrated the strongest antibacterial capability. It can be observed that untreated Sep materials did not show a significant antibacterial effect, indicating the selective antibacterial activities of Sep. It can be inferred that the antibacterial properties of the composites are attributed to the Ag, CuO and ZnO components incorporated into the Sep nanofibres.

The antibacterial mechanism of the Sep composites is presented in Fig. 7. For example, Sep/Ag composites release Ag ions in a sustained manner (Abad-Álvaro *et al.*, 2019; Li *et al.*, 2022). Positively charged Ag ions interact with negatively charged cell membranes due to electrostatic attraction (Domínguez *et al.*, 2021). The denaturation of proteins causes the cell membrane to become permeable and further damages the membrane structure. The accumulated ions within the cells tend to bind with DNA, RNA and other cellular components, hindering genomic replication and ultimately causing bacterial damage (Dos Santos *et al.*, 2014; Briffa *et al.*, 2020). In addition, reactive oxygen species induced by the nanoparticles cause oxidative stress in the bacterial cell, resulting in cellular inactivation (Li *et al.*, 2012). Sep nanofibres play a crucial role in the process mentioned above. Sep improves the dispersion of nanoparticles, and Sep nanofibres anchored with nanoparticles can directly react with bacteria. In this way, the presence of nanoparticles improves the antimicrobial activity of Sep.

The antimicrobial activity and hydrophilicity of Sep composites make them ideal for creating medicated dressings.

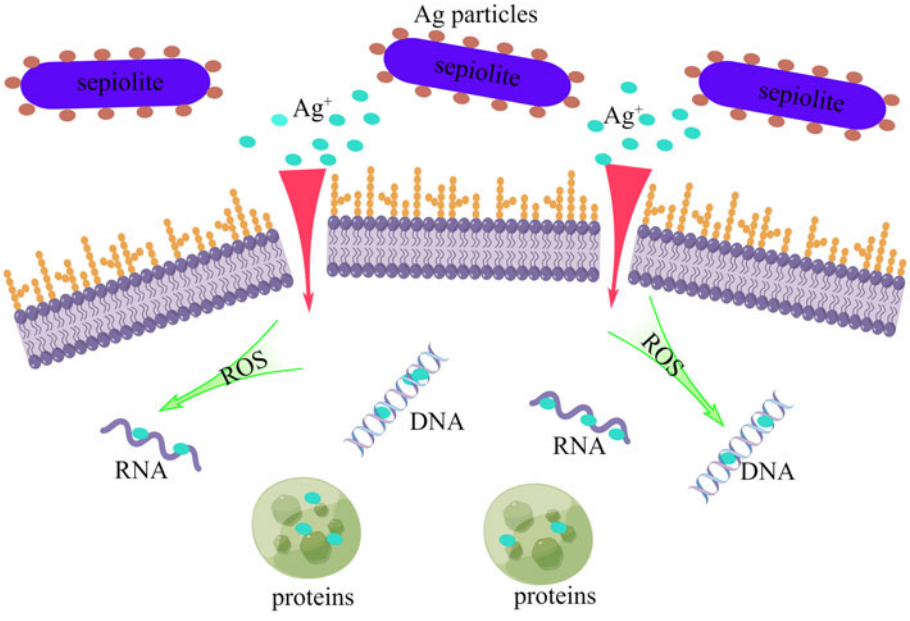

Figure 7. Antibacterial mechanism of the Sep composites. ROS = reactive oxygen species.

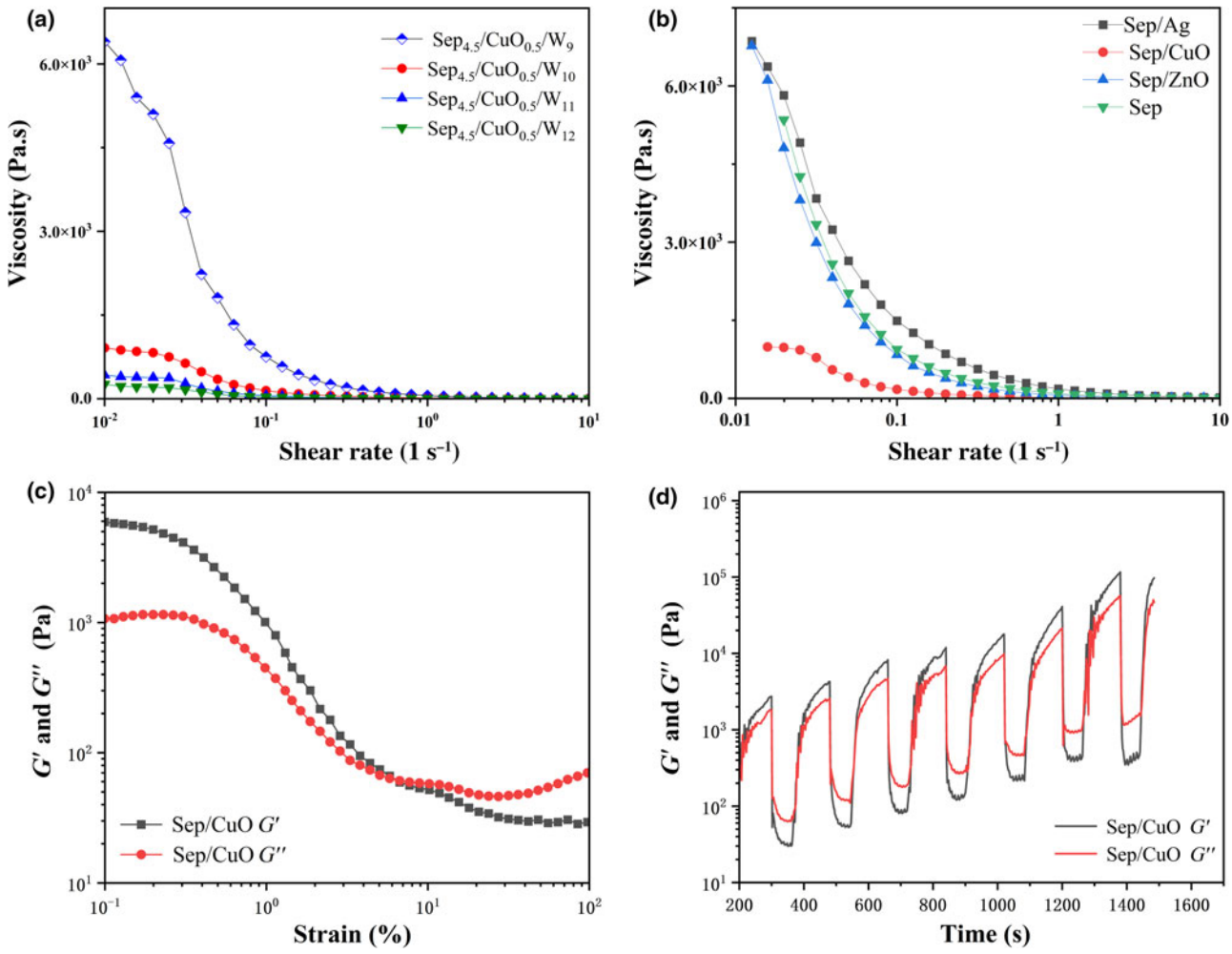

Figure 8. Rheological properties of the mud-like Sep composite mixtures. (a) Viscosity of the Sep/CuO composite at various shear rates. W = water. (b) Viscosity of the various composites at various shear rates. (c) G' and G'' of the Sep/CuO composite on strain sweep. (d) Dynamic strain amplitude cyclic test ($\gamma = 1\%$ for 120 s and $\gamma = 80\%$ for 60 s) of the Sep/CuO composite.

Workability and water retention are critical for the effectiveness of medicated dressings. Thus, the rheological properties of the mud-like Sep composite mixtures were investigated. Figure 8a illustrates the relationship between the water content and the viscosity of composite mixtures, which are formulated with a fixed proportion of Sep and CuO, demonstrating their signature pseudoplastic flow characteristics (Katoueizadeh *et al.*, 2021). The dynamic viscosity of the composites decreased with increasing shear rate, indicating shear-thinning behaviour. As the water content increased, the viscosity of the composites decreased rapidly. The high water retention capacity of Sep ensures that the workability of the composites is preserved only at the optimal water content level (Jiang *et al.*, 2023). Beyond this point, further increasing the water content led to a gradual decrease in viscosity. The data reveal that the Sep/Ag and Sep/ZnO composites exhibit similar rheological properties to pure Sep. In contrast, the Sep/CuO composite shows lower viscosity. This difference may be due to the larger particle size of the components within the Sep/CuO composite (Pastoriza-Gallego *et al.*, 2011; Hu *et al.*, 2020). As shown in Fig. 8c, with increasing strain rate, the storage modulus (G') gradually decreases, whereas the loss modulus (G'') first decreases and then slightly increases. Interestingly, it can be observed that the Sep/CuO composite exhibits very rapid recovery of its mechanical properties after a large-amplitude oscillatory shear deformation (Fig. 8d), known as thixotropy (Wang *et al.*, 2010; Jiao *et al.*, 2021). This indicates that the hydrated Sep/CuO composite exhibits great structural stability. When the strain returns from $\gamma = 80\%$ to 1%, the sample can recover its high dispersibility within ~25 s. During the cycling tests, the G' and G'' of the hydrated Sep/CuO composite gradually increase due to the accelerated evaporation of the water in the system. However, the materials consistently maintained their thixotropic properties, demonstrating the stability of their structural rheological behaviour. The workability of the Sep/CuO composite as medicated dressings is demonstrated in Fig. S6. In the absence of thickeners and water-retaining agents, the hydrated Sep/CuO composite exhibits good adherence to the hydrophilic glass substrates. After 30 min, the mixture did not show significant flow behaviour when the bottles were inverted. For comparison, the mixture exhibits the best workability with a composite/water mass ratio of 1:2.

Conclusion

In summary, Sep-based nanocomposites with improved antibacterial properties have been successfully synthesized using a modified solid-state sintering method. Sep/Ag, Sep/CuO and Sep/ZnO

composites can be synthesized at relatively low temperatures (<500°C). All of the composites exhibit a fibrous morphology, retaining the characteristic structure of pristine Sep. Amongst them, the Sep/Ag composite demonstrates the most potent antibacterial activity, following by CuO- and ZnO-modified Sep composites. The antibacterial rate of the Sep/Ag composite approaches ~100%. In the absence of thickeners and water-retaining agents, the hydrated Sep-based composites exhibit good rheological properties. The hydrated Sep/CuO composite can firmly adhere to hydrophilic glass surfaces. The high water retention of the composites ensures good skin compatibility, making them suitable for direct application to skin. Compared with conventional clay hydrogels, the Sep composites show better antibacterial performance and workability. The results suggest that these composites hold significant potential for clinical use, particularly in the development of wound dressings. This work has promoted the application of clays in the field of biomaterials. Future work needs to further clarify whether clay composites have a promoting effect on wound healing.

Supplementary material. To view supplementary material for this article, please visit https://doi.org/10.1180/clm.2024.13.

Acknowledgements. The authors would like to thank SCI-GO lab (www.sci-go.com) for the XRD, SEM and TEM analysis.

Financial support. This work was supported by Scientific Research Project of Education Department of Hunan Province (22A0113) and Major Science and Technology Projects of Xiangtan Science and Technology Bureau (GX-ZD202210011).

Conflicts of interests. The authors declare that they have no known competing financial interests or personal relationships that could have appeared to influence the work reported in this paper.

Data availability. The datasets used and/or analysed during the current study are available from the corresponding author on reasonable request.

Ethical standards. None.

Author contributions. YY and YD and designed the project and experiments. YJ and ZP prepared the materials and conducted the biological experiments. YL, YT and ZP analysed the results and wrote the manuscript and YD revised the manuscript.

References

Abad-Álvaro I., Trujillo C., Bolea E., Laborda F., Fondevila M., Latorre M. & Castillo J. (2019) Silver nanoparticles–clays nanocomposites as feed additives: characterization of silver species released during *in vitro* digestions. Effects on silver retention in pigs. *Microchemical Journal*, **149**, 104040.

Alves L., Ferraz E., Santarén J., Rasteiro M.G. & Gamelas J.A.F. (2020) Improving colloidal stability of sepiolite suspensions: effect of the mechanical disperser and chemical dispersant. *Minerals*, **10**, 779.

Aranda P. & Ruiz-Hitzky E. (2018) Immobilization of nanoparticles on fibrous clay surfaces: towards promising nanoplatforms for advanced functional applications. *The Chemical Record*, **18**, 1125–1137.

Benli B. & Yalın C. (2017) The influence of silver and copper ions on the antibacterial activity and local electrical properties of single sepiolite fiber: a conductive atomic force microscopy (C-AFM) study. *Applied Clay Science*, **146**, 449–456.

Briffa J., Sinagra E. & Blundell R. (2020) Heavy metal pollution in the environment and their toxicological effects on humans. *Heliyon*, **6**, e04691.

Chen M., Wang D. & Liu X. (2016) Direct synthesis of size-tailored bimetallic Ag/Au nano-spheres and nano-chains with controllable compositions by laser ablation of silver plate in $HAuCl_4$ solution. *RSC Advances*, **6**, 9549–9553.

Chivrac F., Pollet E., Schmutz M. & Avérous L. (2010) Starch nano-biocomposites based on needle-like sepiolite clays. *Carbohydrate Polymers*, **80**, 145–153.

Díez B., Santiago-Morales J., Martínez-Bueno M.J., Fernández-Alba A.R. & Rosal R. (2017) Antimicrobial organic–inorganic composite membranes including sepiolite-supported nanometals. *RSC Advances*, **7**, 2323–2332.

Dikmen S., Yilmaz G., Yorukogullari E. & Korkmaz E. (2012) Zeta potential study of natural- and acid-activated sepiolites in electrolyte solutions. *Canadian Journal of Chemical Engineering*, **90**, 785–792.

Ding Y., Deng C. & Peng J. (2023) A new strategy for preparation of copper oxides composites as anode materials for Li-ion storage. *Solid State Ionics*, **394**, 116195.

Ding Y., Sun J. & Liu X. (2019) Carbon-decorated flower-like ZnO as high-performance anode materials for Li-ion batteries. *Ionics*, **25**, 4129–4136.

Domínguez M., Zarzuela R., Moreno-Garrido I., Carbú M., Cantoral J.M., Mosquera M.J. & Gil M.A. (2021) Anti-fouling nano-Ag/SiO_2 ormosil treatments for building materials: the role of cell-surface interactions on toxicity and bioreceptivity. *Progress in Organic Coatings*, **153**, 106120.

Dos Santos C.A., Seckler M.M., Ingle A.P., Gupta I., Galdiero S., Galdiero M. *et al.* (2014) Silver nanoparticles: therapeutical uses, toxicity, and safety issues. *Journal of Pharmaceutical Sciences*, **103**, 1931–1944.

Dutta J. & Devi N. (2021) Preparation, optimization, and characterization of chitosan–sepiolite nanocomposite films for wound healing. *International Journal of Biological Macromolecules*, **186**, 244–254.

Esteban-Cubillo A., Pecharromán C., Aguilar E., Santarén J. & Moya J.S. (2006) Antibacterial activity of copper monodispersed nanoparticles into sepiolite. *Journal of Materials Science*, **41**, 5208–5212.

Franco F., Pozo M., Cecilia J.A., Benítez-Guerrero M., Pozo E. & Martín Rubí J.A. (2014) Microwave assisted acid treatment of sepiolite: the role of composition and 'crystallinity'. *Applied Clay Science*, **102**, 15–27.

García N., Guzmán J., Benito E., Esteban-Cubillo A., Aguilar E., Santarén J. & Tiemblo P. (2011) Surface modification of sepiolite in aqueous gels by using methoxysilanes and its impact on the nanofiber dispersion ability. *Langmuir*, **27**, 3952–3959.

Hardt J.C., Galdioli Pellá M.C., Reis Meira A.C., Giombelli Rosenberger A., Caetano J. & Cardoso Dragunski D. (2021) Potential wound dressings from electrospun medicated poly(butylene-adipate-co-terephthalate)/poly-(ϵ-caprolactone) microfibers. *Journal of Molecular Liquids*, **339**, 116694.

Hu X., Yin D., Chen X. & Xiang G. (2020) Experimental investigation and mechanism analysis: effect of nanoparticle size on viscosity of nanofluids. *Journal of Molecular Liquids*, **314**, 113604.

Huang X., Hu B., Zhang X., Fan P., Chen Z. & Wang S. (2024) Recent advances in the application of clay-containing hydrogels for hemostasis and wound healing. *Expert Opinion on Drug Delivery*. 10.1080/17425247.2024.2329641.

Jiang W., Han Y., Jiang Y., Xu F., Ouyang D., Sun J. *et al.* (2021) Preparation and electrochemical properties of sepiolite supported Co_3O_4 nanoparticles. *Applied Clay Science*, **203**, 106020.

Jiang W., Jiang Y., Zhao S., Peng J., Qin W., Ouyang D. & Ding Y. (2020) Novel sepiolite-based materials for lithium- and sodium-ion storage. *Energy Technology*, **8**, 1901262.

Jiang Y., Wang L., Qi W., Yin P., Liao X., Luo Y. & Ding Y. (2024) Antibacterial and self-healing sepiolite-based hybrid hydrogel for hemostasis and wound healing. *Biomaterials Advances*, **159**, 213838.

Jiang Y., Yang Y., Peng Z., Li Y., Peng J., Zhang Y. *et al.* (2023) Sustainable sepiolite-based composites for fast clotting and wound healing. *Biomaterials Advances*, **149**, 213402.

Jiao Y., Lu Y., Lu K., Yue Y., Xu X., Xiao H. *et al.* (2021) Highly stretchable and self-healing cellulose nanofiber-mediated conductive hydrogel towards strain sensing application. *Journal of Colloid and Interface Science*, **597**, 171–181.

Junior H.B., da Silva E., Saltarelli M., Crispim D., Nassar E.J., Trujillano R. *et al.* (2020) Inorganic–organic hybrids based on sepiolite as efficient adsorbents of caffeine and glyphosate pollutants. *Applied Surface Science Advances*, **1**, 100025.

Katoueizadeh E., Rasouli M. & Zebarjad S.M. (2021) The rheological behavior of the non-Newtonian thixotropic colloidal silica gels from sodium silicate. *Materials Chemistry and Physics*, **272**, 124994.

Kose A., Karabagli Y., Kurkcuoglu M. & Cetin C. (2005). Alpha sepiolite: an old clay mineral – a new dressing material. *Wounds – A Compendium of Clinical Research and Practice*, **17**, 114–121.

Li D., Liu P., Hao F., Lv Y., Xiong W., Yan C. & Wu Y. (2022) Preparation and application of silver/chitosan–sepiolite materials with antimicrobial activities and low cytotoxicity. *International Journal of Biological Macromolecules*, **210**, 337–349.

Li Y., Zhang W., Niu J. & Chen Y. (2012) Mechanism of photogenerated reactive oxygen species and correlation with the antibacterial properties of engineered metal-oxide nanoparticles. *ACS Nano*, **6**, 5164–5173.

Lisuzzo L., Wicklein B., Dico G.L., Lazzara G., Del Real G., Aranda P. & Ruiz-Hitzky E. (2020) Functional biohybrid materials based on halloysite, sepiolite and cellulose nanofibers for health applications. *Dalton Transactions*, **49**, 3830–3840.

Liu M., He R., Yang J., Long Z., Huang B., Liu Y. & Zhou C. (2016) Polysaccharide–halloysite nanotube composites for biomedical applications: a review. *Clay Minerals*, **51**, 457–467.

Liu R., Ji Z., Wang J. & Zhang J. (2018) Solvothermal fabrication of TiO_2/sepiolite composite gel with exposed {0 0 1} and {1 0 1} facets and its enhanced photocatalytic activity. *Applied Surface Science*, **441**, 29–39.

Ma Y. & Zhang G. (2016) Sepiolite nanofiber-supported platinum nanoparticle catalysts toward the catalytic oxidation of formaldehyde at ambient temperature: efficient and stable performance and mechanism. *Chemical Engineering Journal*, **288**, 70–78.

Pang Y., Yu Z., Chen H., Xiang Q., Wang Q., Xie C. & Liu Y. (2022) Superhydrophobic polyurethane sponge based on sepiolite for efficient oil/water separation. *Journal of Hazardous Materials*, **434**, 128833.

Pastoriza-Gallego M.J., Casanova C., Legido J.L. & Piñeiro M.M. (2011) CuO in water nanofluid: influence of particle size and polydispersity on volumetric behaviour and viscosity. *Fluid Phase Equilibria*, **300**, 188–196.

Song J., Ren X., Hu G., Hu X. & Cheng W. (2023) Enhanced PMS activation by MOF-derived Co_3O_4/sepiolite composite for norfloxacin degradation: performance, mechanism and degradation pathway. *Process Safety and Environmental Protection*, **176**, 140–154.

Tavakoli J. (2017) Physico-mechanical, morphological and biomedical properties of a novel natural wound dressing material. *Journal of the Mechanical Behavior of Biomedical Materials*, **65**, 373–382.

Uygun O., Murat A. & Çakal G.Ö. (2023) Magnetic sepiolite/iron(III) oxide composite for the adsorption of lead(II) ions from aqueous solutions. *Clay Minerals*, **58**, 267–279.

Valentín J.L., López-Manchado M.A., Rodríguez A., Posadas P. & Ibarra L. (2007) Novel anhydrous unfolded structure by heating of acid pre-treated sepiolite. *Applied Clay Science*, **36**, 245–255.

Vilarrasa-García E., Cecilia J.A., Bastos-Neto M., Cavalcante C.L., Azevedo D.C.S. & Rodríguez-Castellón E. (2017) Microwave-assisted nitric acid treatment of sepiolite and functionalization with polyethylenimine applied to CO_2 capture and CO_2/N_2 separation. *Applied Surface Science*, **410**, 315–325.

Wang Q., Mynar J.L., Yoshida M., Lee E., Lee M., Okuro K. *et al.* (2010) High-water-content mouldable hydrogels by mixing clay and a dendritic molecular binder. *Nature*, **463**, 339–343.

Wang Q., Tang A., Zhong L., Wen X., Yan P. & Wang J. (2018) Amino-modified γ-Fe_2O_3/sepiolite composite with rod-like morphology for magnetic separation removal of Congo Red dye from aqueous solution. *Powder Technology*, **339**, 872–881.

Wu X., Zhang Q., Liu C., Zhang X. & Chung D.D.L. (2017) Carbon-coated sepiolite clay fibers with acid pre-treatment as low-cost organic adsorbents. *Carbon*, **123**, 259–272.

Yang F. & Wang A. (2022) Recent researches on antimicrobial nanocomposite and hybrid materials based on sepiolite and palygorskite. *Applied Clay Science*, **219**, 106454.

Zhang G, Xiao Y, Yin Q, Yan J, Zang C, Zhang H. (2021a) *In situ* synthesis of silver nanoparticles on amino-grafted polyacrylonitrile fiber and its antibacterial activity. *Nanoscale Research Letters*, **16**, 36.

Zhang W., Wu J., Yu L., Chen H., Li D., Shi C. *et al.* (2021b) Paraffin-coated hydrophobic hemostatic zeolite gauze for rapid coagulation with minimal adhesion. *ACS Applied Materials & Interfaces*, **13**, 52174–52180.

Zhang Y., Wang D. & Zhang G. (2011) Photocatalytic degradation of organic contaminants by TiO_2/sepiolite composites prepared at low temperature. *Chemical Engineering Journal*, **173**, 1–10.

Zheng L., Li X., Xu C., Xu Y., Zeng Y., Tam M. *et al.* (2023) High-efficiency antibacterial hemostatic AgNP@zeolite/chitin/bamboo composite sponge for wound healing without heat injury. *Advanced Healthcare Materials*, **12**, 2300075.

Zhou F., Yan C., Liang T., Sun Q. & Wang H. (2018) Photocatalytic degradation of Orange G using sepiolite–TiO_2 nanocomposites: optimization of physicochemical parameters and kinetics studies. *Chemical Engineering Science*, **183**, 231–239.

Zhou J., Jiang W., Peng J. & Ding Y. (2022) An environmentally friendly sepiolite/Cu_2O/Cu ternary composite as anode material for Li-ion batteries. *Ionics*, **28**, 1091–1098.

Zhou J., Wang Z., Alcântara A.C.S. & Ding Y. (2023) Study of the adsorption mechanisms of NH_3, H_2S and SO_2 on sepiolite using molecular dynamics simulations. *Clay Minerals*, **58**, 1–6.